Electronic Supplementary Material (ESI) for Journal of Materials Chemistry C.

Supporting Information

Centimeter-size single crystal of a lead-free double perovskite for broad-spectrum polarization-sensitive detection

Zhou Li, [ab] Qin Chen,[ab] Ziyang Wang,[b] Yipeng Fan,[ab] Tingting Zhu,[b] Chengmin Ji* [b], Xiaojun Kuang* [a] and Junhua Luo* [b]

a.School of Chemistry and Biological Engineering (Guangxi Key Laboratory of Electrochemical and Magnetochemical Functional Materials), Guilin University of Technology, Guangxi, Guilin 541004 (China)
b.State Key Laboratory of Structural Chemistry, Fujian Institute of Research on the Structure of Matter, Chinese Academy of Sciences, Fuzhou, Fujian 35002 (China).
*E-mail: jhluo@fjirsm.ac.cn, kuangxj@glut.edu.cn, cmji@fjirsm.ac.cn.

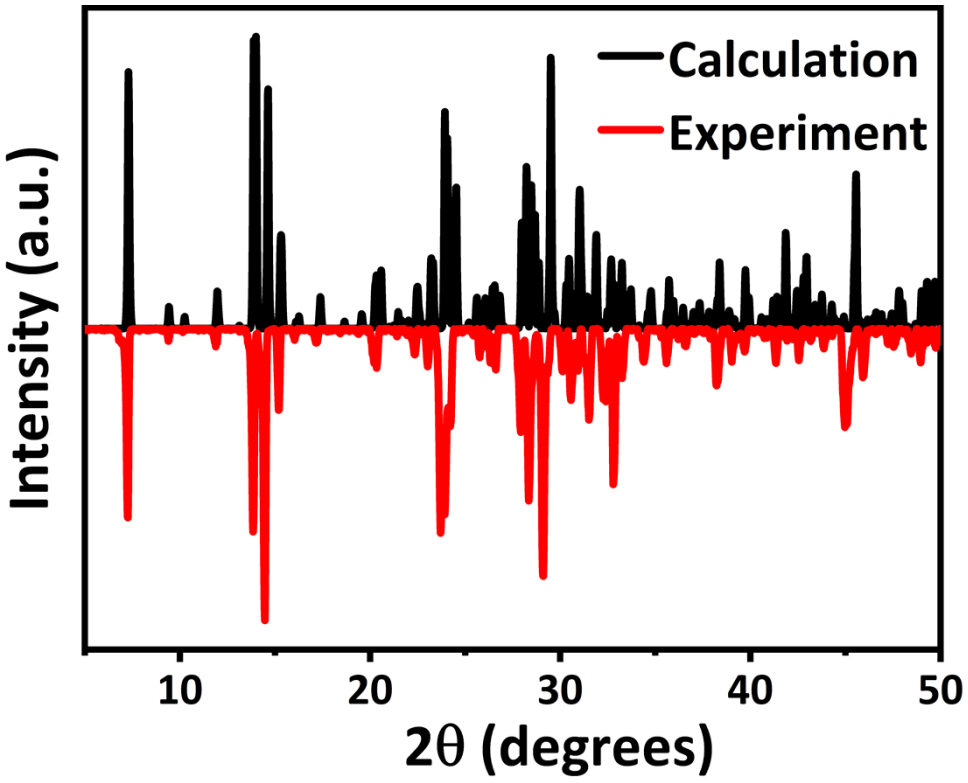

Figure S1 Experimental and simulated X-ray powder diffraction patterns for $(IPA)_4AgBiI_8$.

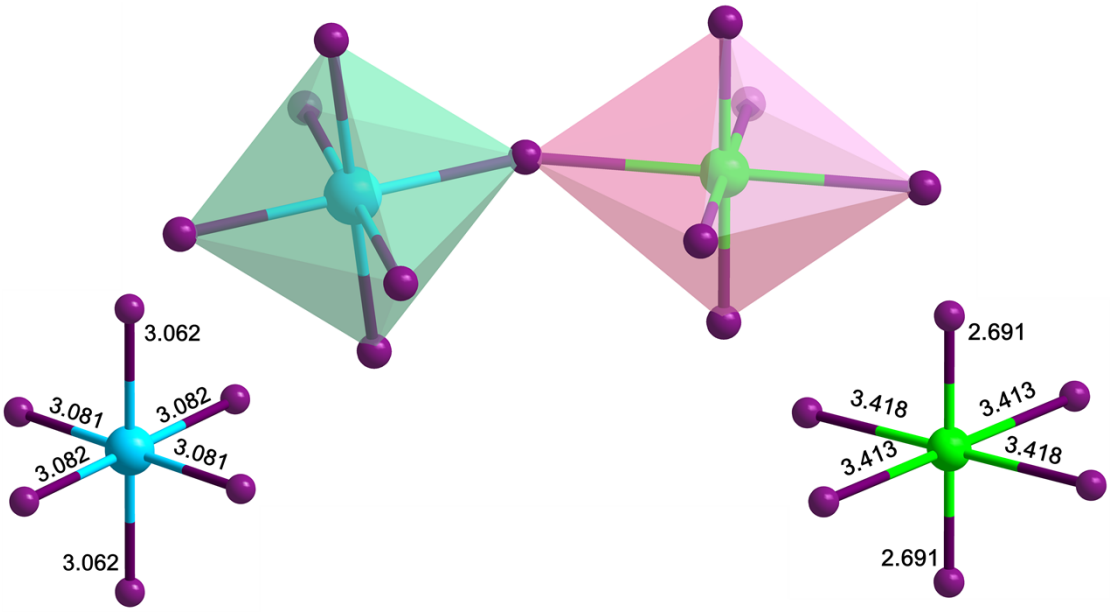

Figure S2. Two inhomogeneous octahedral configuration of BiI_6 and AgI_6 octahedra.

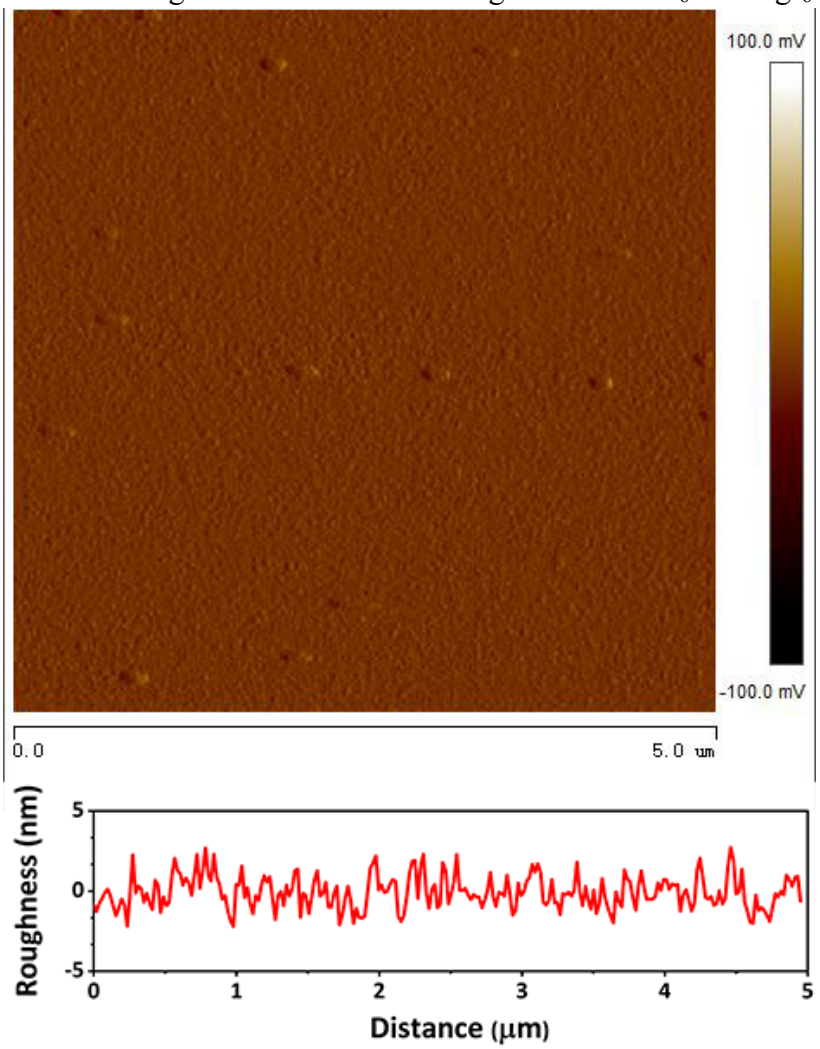

Figure S3. AFM image measured on the surface of single crystal of $(IPA)_4AgBiI_8$.

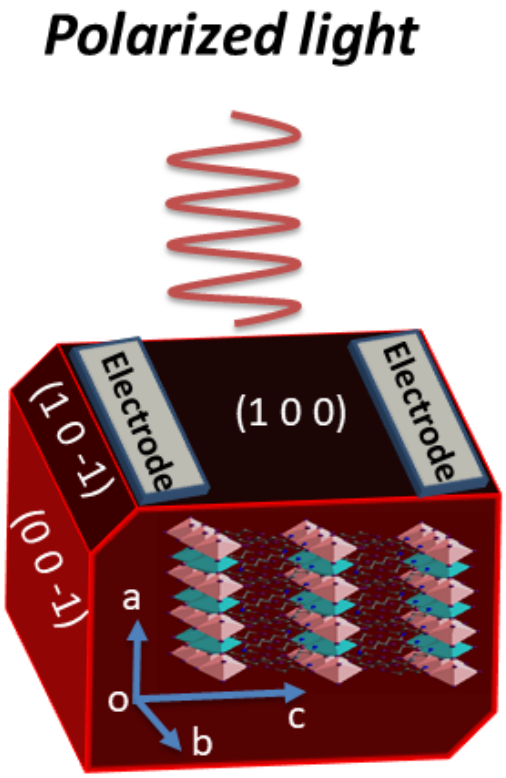

Figure S4. Schematic diagram for crystal-based detector.

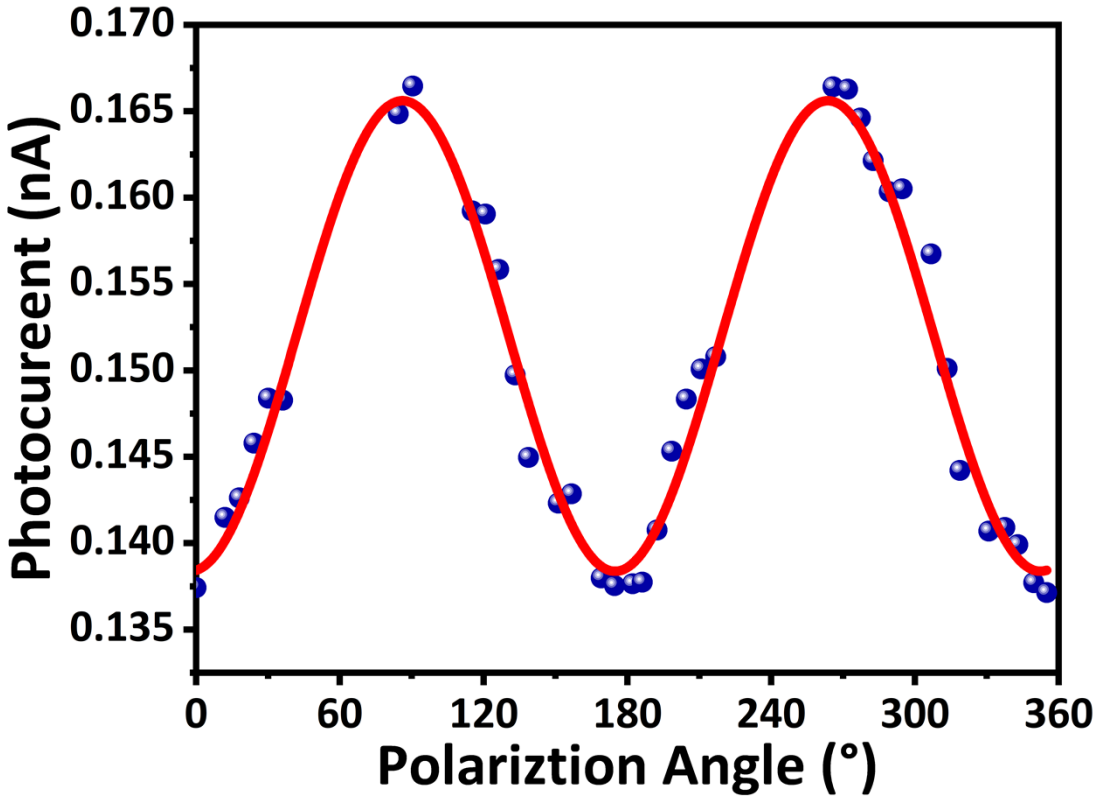

Figure S5. Polarized photoelectric test of $(IPA)_4AgBiI_8$.

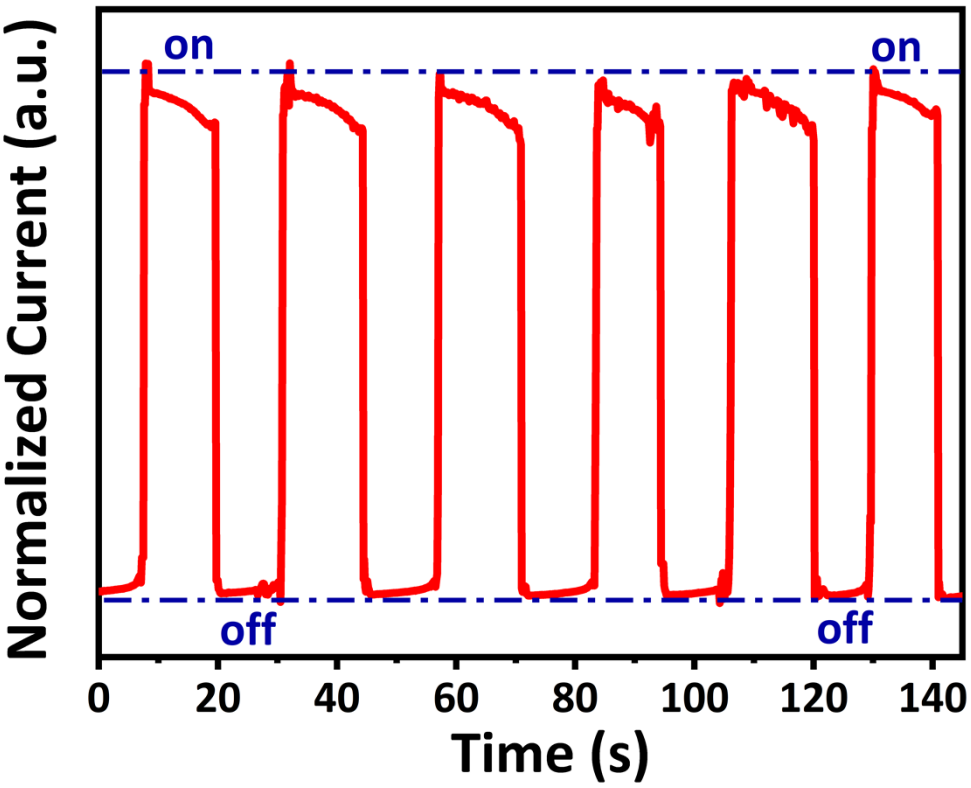

Figure S6. At 10 V bias, time-dependent switching cycles of photocurrent response for $(IPA)_4AgBiI_8$.

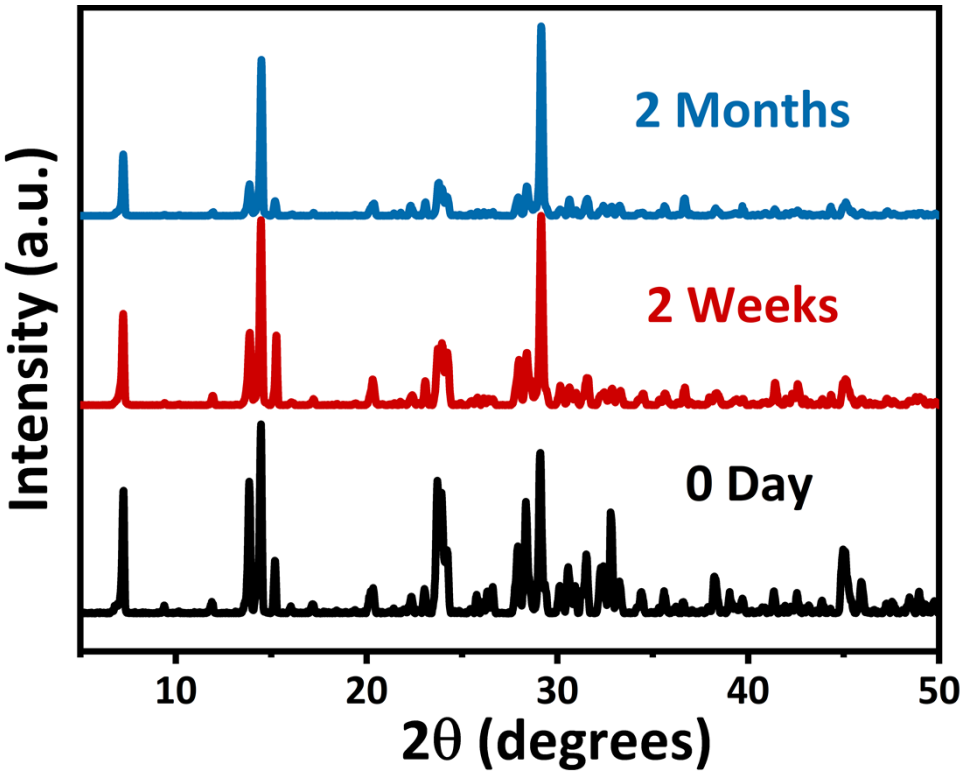

Figure S6. The PXRD spectra of (IPA)4AgBiI8 powder and the simulated single crystal structure for comparison.

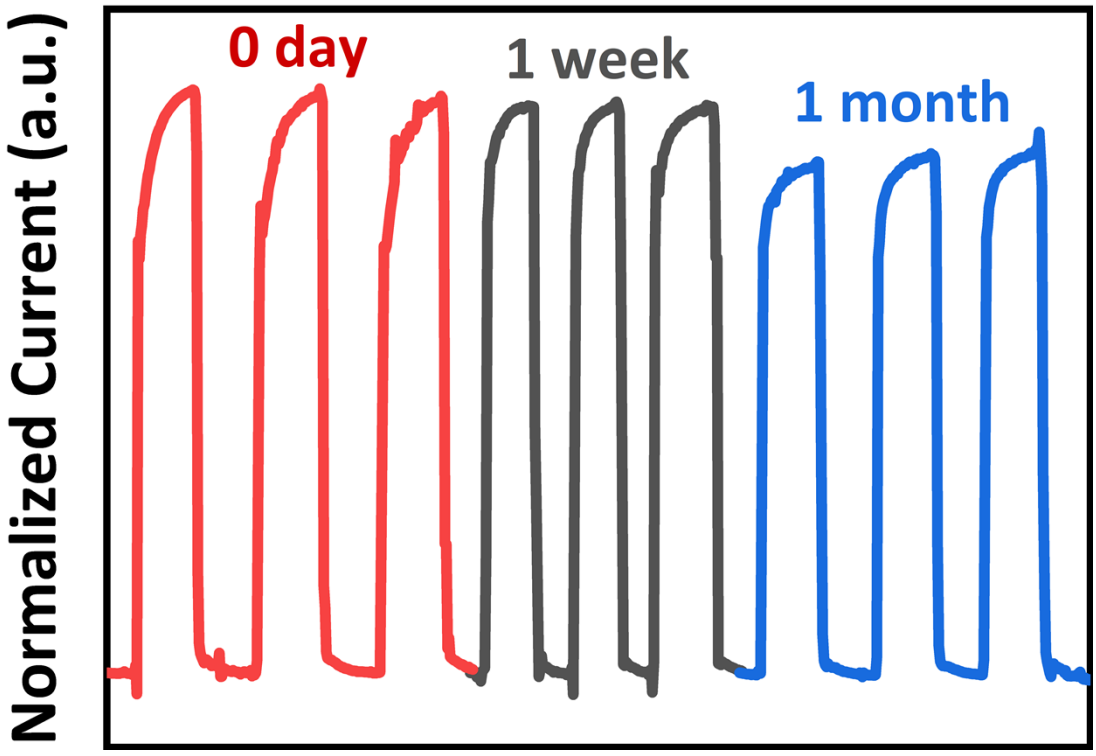

Figure S8. The stability of photoelectric properties of $(IPA)_4AgBiI_8$.

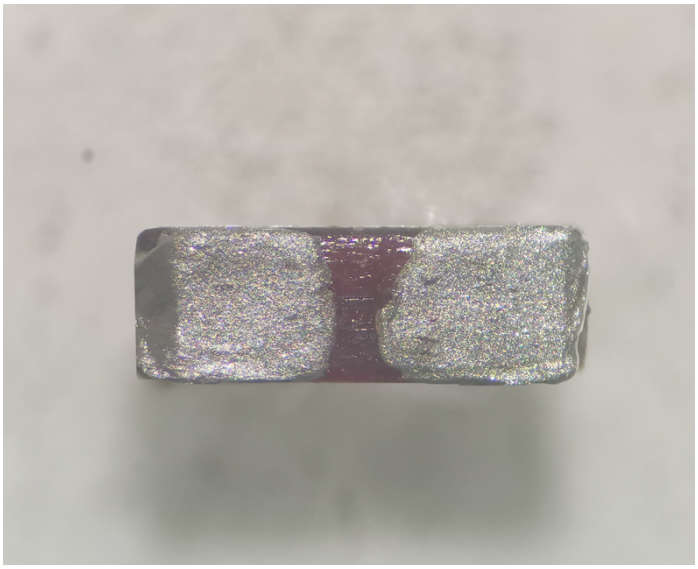

Figure S9. The electrode equipment photo.

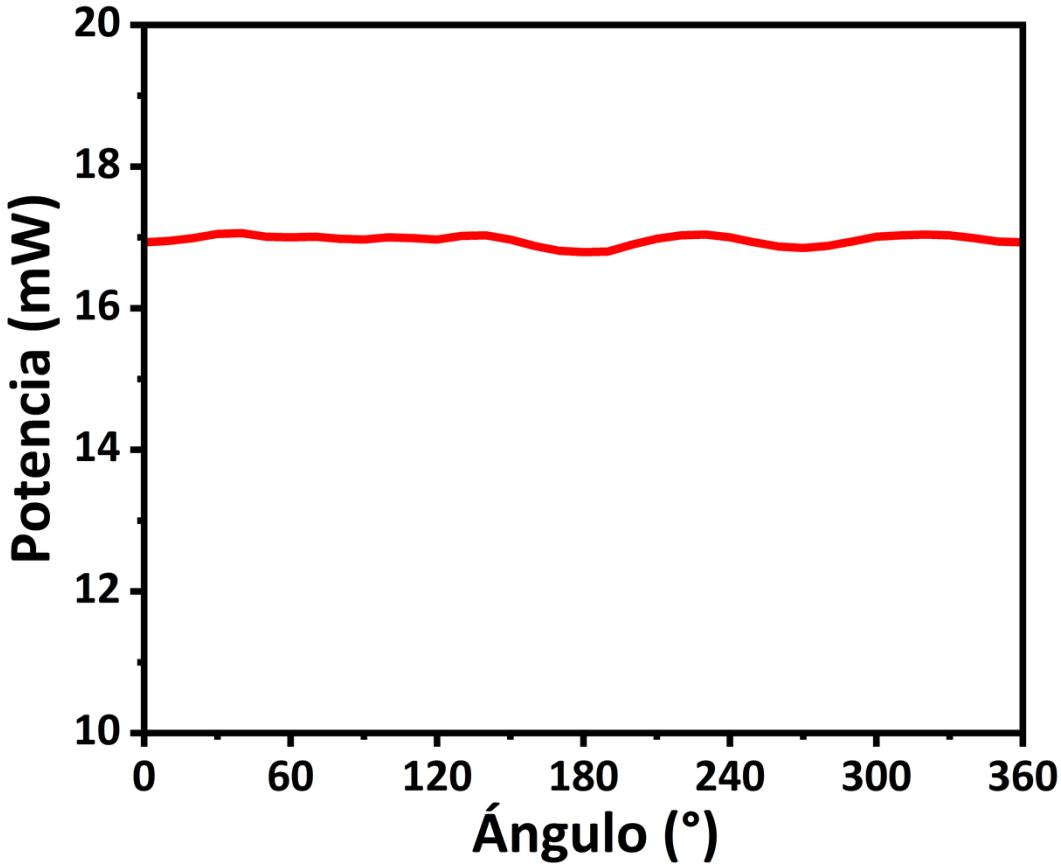

Figure S10. The light intensity at different polarization angles

Table S1 Crystal data for $(IPA)_4AgBiI_8$. collected at 300 K.

Empirical formula	$C_{12}H_{36}AgBiI_{12}N_4$
Formula weight	2076.10
Temperature/K	299.92
Crystal system	triclinic
Space group	P-1
Cell parameters	a=8.7529(4)
	b=9.4129(5)
	C=12.3100(7)
V(Å^3)	1010.13(9)
Z,ρ_{cal}. (g/cm^3)	1
F(000)	902.0
2Theta range(°)	5.436 to 55.136
Limiting indices	$-11 \leq h \leq 11$
	$-12 \leq k \leq 12$
	$-16 \leq l \leq 16$
Reflections collected	29963
Independent reflections	4652 [R_{int}= 0.0618, R_{sigma}= 0.0383]
Data/restraints/parameters	4652/0/142
GOF	1.050
Final R indexes [I>=2σ (I)]	R_1 = 0.0472, wR_2 = 0.1492
Final R indexes [all data]	R_1 = 0.0517, wR_2 = 0.1546

Table S2 The optical band gaps of typical halide double perovskites.

Compound	Band gap (eV)	Optical absorption cutoff (nm)	Ref.
$Cs_2AgBiBr_6$	2.20	550	1
$MA_2AgBiBr_6$	2.00	597	1
MA_2AgBiI_6	1.64		1
$(i\text{-PA})_2CsAgBiBr_7$	2.85	526	2
$(BA)_2CsAgBiBr_7$	2.40	522	3
$(3AMPY)_2AgBiI_8 \cdot H_2O$	1.86	675	4
$(C_6H_{16}N_2)_2AgBiI_8 \cdot H_2O$	1.93		5
$[AE2T]_2AgBiI_8$	2.00		6
$[(R)\text{-}\beta\text{-MPA}]_4AgBiI_8$	2.01	616	7
$(4,4\text{-difluoropiperidinium})_4AgBiI_8$	2.03		8
$(IPA)_4gBiI_8$	1.87	660	Our work

1. S. M. Saeed; A. Hossein; G. M. Reza, *Materials Science in Semiconductor Processing*, 2021, **125**, 105639.
2. Y. Li; T. Yang; Z. Xu; X. Liu; X. Huang; S. Han; Y. Liu; M. Li; J. Luo; Z. Sun, *Angew Chem Int Ed Engl*, 2020, **59**, 3429.
3. Z. Xu; X. Liu; Y. Li; D. X. Liu; T. Yang; C. Ji; S. Han; P. Y. Xu; P. J. Luo; P. Z. Sun, *Angewandte Chemie*, 2019, **131**, 15757.
4. D. Fu; S. Wu; Y. Liu; Y. Yao; Y. He; X.-M. Zhang, *Inorganic Chemistry Frontiers*, 2021, **8**, 3576.
5. L. Y. Bi; Y. Q. Hu; M. Q. Li; T. L. Hu; H. L. Zhang; X. T. Yin; W. X. Que; M. S. Lassoued; Y. Z. Zheng, *J Mater Chem A*, 2019, **7**, 19662.
6. M. K. Jana; S. M. Janke; D. J. Dirkes; S. Dovletgeldi; C. Liu; X. X. Qin; K. Gundogdu; W. You; V. Blum; D. B. Mitzi, *Journal of the American Chemical Society*, 2019, **141**, 7955.
7. D. Li; X. Liu; W. Wu; Y. Peng; S. Zhao; L. Li; M. Hong; J. Luo, *Angewandte Chemie-International Edition*, 2021, **60**, 8415.
8. C. F. Wang; H. J. Li; M. G. Li; Y. Cui; X. Son; Q. W. Wang; J. Y. Jiang; M. M. Hua; Q. Xu; K. Zhao; H. Y. Ye; Y. Zhang, *Advanced Functional Materials*, 2021, **31**, 2009457.